Synthesis and Molecular Modeling Studies of SYNPHOS®, a New, Efficient Diphosphane Ligand For Ruthenium-Catalyzed Asymmetric Hydrogenation

Sébastien Duprat de Paule,[a] Séverine Jeulin,[a] Virginie Ratovelomanana-Vidal,*[a] Jean-Pierre Genêt,*[a] Nicolas Champion,[b] and Philippe Dellis[b]

Keywords: Asymmetric catalysis / Atropisomerism / Hydrogenation / Molecular modeling / Phosphanes / Ruthenium

A new, optically active, atropisomeric diphosphane ligand, (2,3,2′,3′-tetrahydro-5,5′-bi(1,4-benzodioxin)-6,6′-diyl)bis-(diphenylphosphane) (SYNPHOS®), has been synthesized, characterized, and used in ruthenium-catalyzed asymmetric hydrogenations. This new ligand has been compared with other atropisomeric diphosphanes (BINAP and MeO-BIPHEP) with respect to their dihedral angles calculated by molecular modeling and the enantioselectivity of their ruthenium-mediated hydrogenation reactions.

(© Wiley-VCH Verlag GmbH & Co. KGaA, 69451 Weinheim, Germany, 2003)

Introduction

In the last two decades, considerable effort has been made in the design of new ligands for the development of highly efficient metal-catalyzed asymmetric transformations.[1] Nevertheless, the synthesis and applications of new and effective chiral ligands remain of great importance. Atropisomeric bisphosphane ligands, such as BINAP,[2] MeO-BIPHEP,[3] or SEGPHOS,[4] have high efficiencies when applied to various transition metal-catalyzed reactions,[5] in particular for ruthenium-catalyzed hydrogenation reactions.[6] Structural variations of these ligands can provide new chiral catalysts, with dramatic effects on the enantioselectivities of their catalyzed reactions. Biphenylphosphanes containing oxygenated groups, like MeO-BIPHEP,[7] TUNAPHOS,[8] or SEGPHOS,[9] have exhibited slightly higher enantioselectivities than BINAP. We have recently designed functionalized BINAP-derived ligands, such as *Digm*-BINAP[10a] and MeO-NAPhePHOS,[10b] and in our continuing interest for the synthesis and use of new chiral diphosphane ligands in asymmetric catalysis, we decided to focus on oxygen-containing atropisomeric ligands and study their geometric and electronic properties.

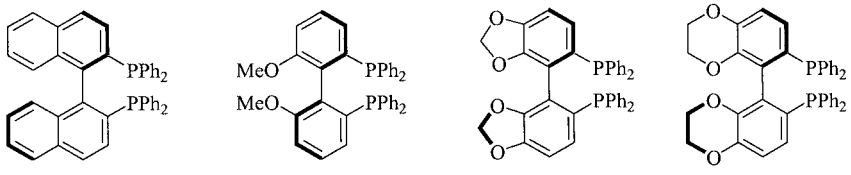

(*R*)-BINAP (*R*)-MeO-BIPHEP (*R*)-SEGPHOS (*R*)-SYNPHOS®

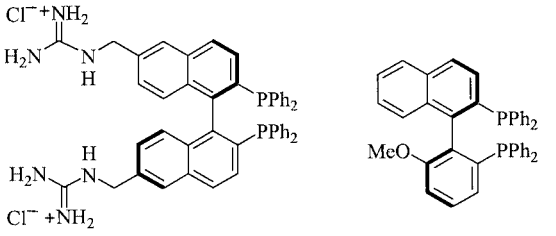

(*R*)-*Digm*-BINAP (*R*)-MeO-NAPhePHOS

[a] Laboratoire de Synthèse Sélective Organique et Produits Naturels, UMR 7573, Ecole Nationale Supérieure de Chimie de Paris,
11 rue P. et M. Curie, 75231 Paris Cedex 05, France
Fax: (internat.) + 33-1/44071062
E-mail: genet@ext.jussieu.fr
gvidal@ext.jussieu.fr
[b] Synkem S.A.S.,
47 rue de Longvic 21301 Chenôve Cedex, France

This paper reports the synthesis of enantiopure (*R*)- and (*S*)-(2,3,2′,3′-tetrahydro-5,5′-bi(1,4-benzodioxin)-6,6′-diyl)-bis(diphenylphosphane) [(*R*)- and (*S*)-SYNPHOS®],[11] structural information on SYNPHOS® derived from its crystal structure and molecular modeling, and a study of the influence of the dihedral angle of diphosphanes on the enantioselectivity of ruthenium-catalyzed hydrogenation reactions.

Results and Discussion

Synthesis of SYNPHOS®

The synthesis of SYNPHOS® was accomplished in a five-step procedure starting from commercial 1,4-benzodioxane. In the first step, 1,4-benzodioxane (**1**) was readily brominated in quantitative yield with *N*-bromosuccinimide in DMF. 6-Bromo-1,4-benzodioxane (**2**) was lithiated by lithium−halogen exchange with 1.1 equivalents of *n*-butyllithium at −78 °C in THF, then reacted with 1.1 equivalents of $ClPPh_2$, and finally oxidized with hydrogen peroxide to afford phosphane oxide **3** as a pale yellow solid in high yields, as depicted in Scheme 1.

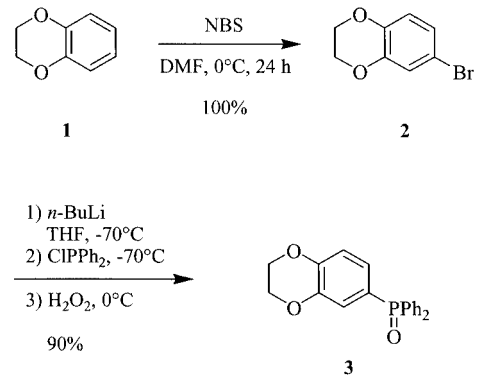

Scheme 1

Dimerization of compound **3** was a key step for the synthesis of SYNPHOS® ligand. We proceeded in two different manners: Ullmann-type coupling with copper and oxidative homo-coupling with iron(III) chloride, as shown in Scheme 2.

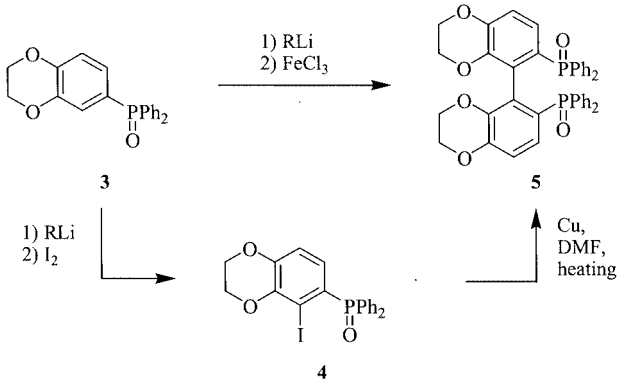

Scheme 2

The first aim was to achieve ortholithiation of compound **3**. The lithiated intermediate could be oxidized by $FeCl_3$ to provide bis(phosphane oxide) **5**, or transformed into an iodide derivative **4** suitable for Ullmann coupling. As outlined in Table 1, we tried several conditions for the difficult ortholithiation/oxidative coupling sequence. Best results were obtained with *t*BuLi at low temperature (−100 °C then −70 °C) under thermodynamically controlled conditions,[12] and compound **5**, hereafter named $SYNPHOSO_2$, was obtained in 50% yield by using $FeCl_3$ as the coupling agent.

Table 1. Ortholithiation conditions for phosphane oxide **3**

RLi	Equiv.	Yield of **5**
LDA, −78 °C, 2 h	1	−
LDA, −50 °C, 2 h	1	−
$LiNEt_2$, −40 °C, 3 h	1.1	−
*n*BuLi/TMEDA, −50 °C, 2 h	1	degradation
*s*BuLi/TMEDA, −60 °C, 3 h	1.2	25%
*n*BuLi, −50 °C, 2 h	3	degradation
*s*BuLi, −50 °C, 2 h	1.1	20%
*t*BuLi, −50 °C, 2 h	1	20%
*t*BuLi, −100 °C then −70 °C, 4 h	1	50%

Using the optimized ortholithiation conditions (*t*BuLi, −100 °C then −70 °C), we achieved the formation of iodide **4** in 75% yield by reaction of the lithiated intermediate with I_2 at −70 °C in THF. The crude iodide was directly subjected to the Ullmann reaction and bis(phosphane oxide) **5** was isolated in 50% yield from compound **3**.

Racemic $SYNPHOSO_2$ was resolved with *O*,*O*-dibenzoyltartaric acid[13] [(+)- or (−)-DBTA] by fractional crystallization, as depicted in Scheme 3. A solution of racemic $SYNPHOSO_2$ in chloroform and a solution of (−)-DBTA in ethyl acetate were mixed at room temperature ($CHCl_3$/EtOAc, 1:3). After a few minutes, precipitation of a 1:1 complex of (−)-DBTA and (−)-$SYNPHOSO_2$ was observed. Treatment of the tartrate complex with aqueous base (1 N KOH) provided enantiomerically enriched (−)-$SYNPHOSO_2$ [*ee* = 70%, according to HPLC (Chiralcel OD-H column)]. Enantiomerically pure (−)-$SYNPHOSO_2$ was obtained in 70% yield, based on the amount of (−)-$SYNPHOSO_2$ in racemic **5**, by repeating this operation four times. Enantiomerically enriched (+)-$SYNPHOSO_2$ was recovered from the mother liquor after treatment with aqueous base. Using a method similar to that described above, enantiomerically pure (+)-$SYNPHOSO_2$ was obtained in 70% yield, based on the amount of (+)-$SYNPHOSO_2$ in racemic **5**, from enantiomerically enriched (+)-**5** by using (+)-DBTA. A better procedure was found: when racemic $SYNPHOSO_2$ and (+)-DBTA were mixed in dichloromethane at room temperature, a 1:1 complex of (+)-DBTA and (−)-$SYNPHOSO_2$ precipitated. Treatment of the tartrate complex with aqueous base (1 N KOH) provided enantiomerically enriched (−)-$SYNPHOSO_2$ (*ee* = 91%). Enantiomerically pure (−)-$SYNPHOSO_2$ was obtained in 90% yield, based on the amount of (−)-$SYNPHOSO_2$ in racemic

 © 2003 Wiley-VCH Verlag GmbH & Co. KGaA, Weinheim

5, by repeating this operation one more time. Interestingly, $SYNPHOSO_2$ with the opposite configuration, compared to that observed from chloroform/ethyl acetate, was obtained using dichloromethane.

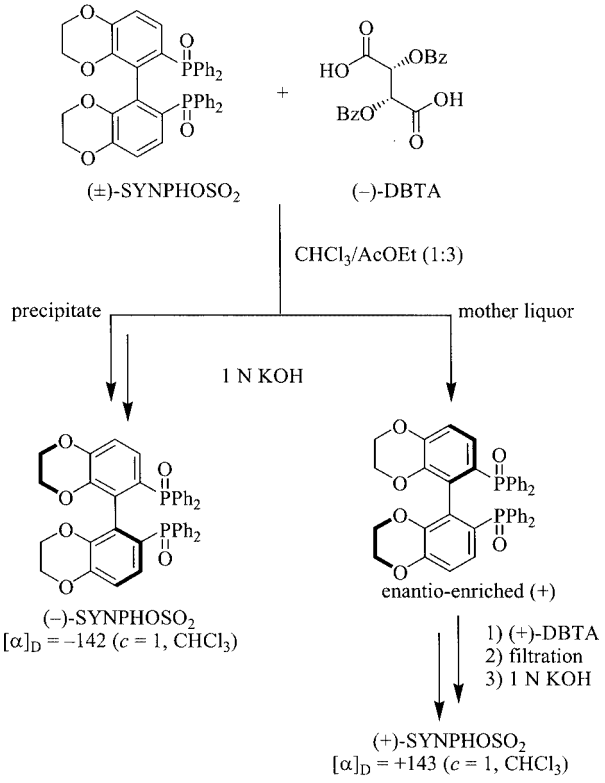

Scheme 3. Resolution of $SYNPHOSO_2$

A 1:1 complex of (−)-$SYNPHOSO_2$ and (−)-DBTA was recrystallized from ethanol, yielding colorless needles suitable for X-ray analysis. The crystal consists of polymeric chains of alternating $SYNPHOSO_2$ and DBTA molecules connected by hydrogen bonds (Figure 1). From the internal comparison with (−)-DBTA, the absolute configuration of (−)-$SYNPHOSO_2$ is unambiguously defined to be (*S*). The two benzodioxane units in $SYNPHOSO_2$ are positioned almost perpendicular to one another with an angle of 84.97° between their planes. The distance between the carboxylic oxygen atom and the oxygen atom on the phosphorus atom is 2.57 Å.

The final step in the synthetic route was the reduction of bis(phosphane oxide) **5**. This transformation was accomplished by treatment of $SYNPHOSO_2$ with trichlorosilane/NBu_3 in refluxing xylene. In this way, (−)-(*S*)- and (+)-(*R*)-SYNPHOS® were obtained after simple precipitation from MeOH with high yields, as depicted in Scheme 4. The enantiomeric purity of the product obtained from this reaction was determined by two complementary methods. HPLC analyses of samples of diphosphanes (−)-(*S*)-**6** and (+)-(*R*)-**6** oxidized with hydrogen peroxide showed that no racemization had occurred during the reduction process. The enantiomeric purity of diphosphanes (−)-(*S*)-**6** and (+)-(*R*)-**6** was also confirmed by the assignment of the ^1H NMR spectral shifts of the palladium complex formed in situ with [(+)-di-μ-chlorobis{2-[(dimethylamino)methyl]phenyl-*C*,*N*}dipalladium] (Scheme 5).[14,15] The appearance of a single set of signals confirmed the enantiomeric purity of the diphosphanes to be > 95%.

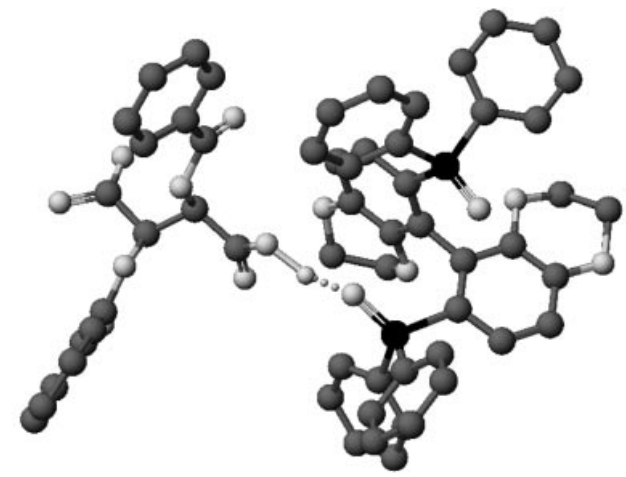

Figure 1. X-ray structure of [(−)-DBTA·(*S*)-**5**] (Chem3D representation, H atoms omitted for clarity)

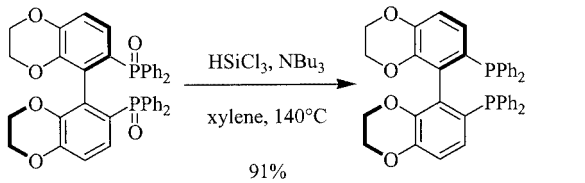

Scheme 4. Reduction of $SYNPHOSO_2$

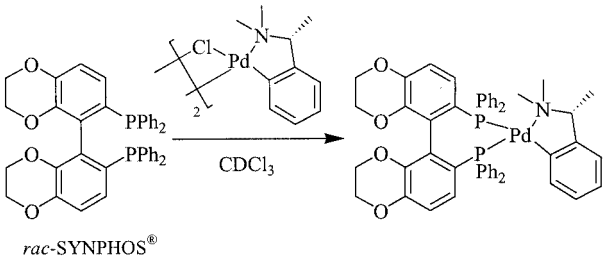

Selected ^1H-NMR data[a] of Pd complexes derived from diphosphane **6**

Diphosphane	NC*H*Me	NCH*Me*	N*Me*$_a$	N*Me*$_b$
(*R*)	5.20 (~ *q*)	1.32 (*d*, 6.5)	2.54 (*t*, 3.5)	1.49 (*d*, 2.5)
(*S*)	3.52 (~ *q*)	2.24 (*d*, 6.5)	2.14 (*m*)	1.89 (br, *s*)

[a] In $CDCl_3$, at 200 MHz; chemical shifts (ppm) relative to TMS (*J* in Hz).

Scheme 5

Asymmetric Hydrogenation

Since the pioneering work of Noyori[16] and Ikariya,[17] ruthenium-catalyzed asymmetric hydrogenation, especially with atropisomeric diphosphane ligands, has become a very convenient method for producing optically active alcohols

 © 2003 Wiley-VCH Verlag GmbH & Co. KGaA, Weinheim

and other chiral building blocks.[6] For some time now, we have been developing an efficient and general procedure for the screening of new ligands in ruthenium-mediated asymmetric hydrogenation.[18]

Following our convenient in situ procedure,[19] catalysts were prepared from commercially available [Ru(COD)(2-methylallyl)$_2$] and SYNPHOS® ligand in acetone by addition of a methanolic solution of HBr, as detailed in Scheme 6. After removal of the solvent in vacuo, these complexes were used without further purification.

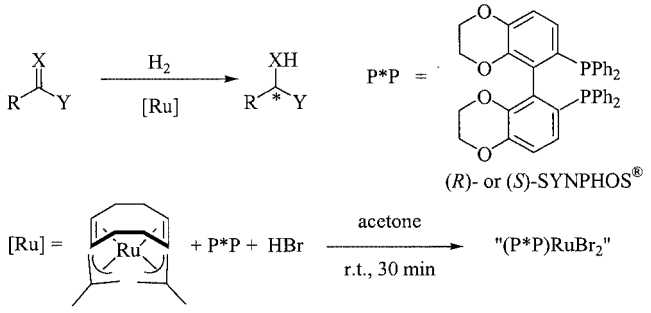

Scheme 6. General procedure for ruthenium-mediated asymmetric hydrogenation reactions using SYNPHOS®

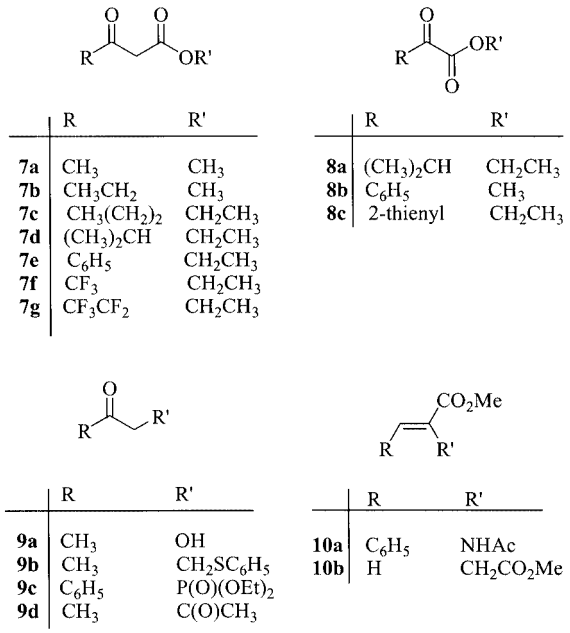

Scheme 7. Hydrogenation substrates

Using SYNPHOS®, we investigated the hydrogenation reaction of various substrates: β-keto esters, α-keto esters, functionalized ketones, and ethylenic compounds, as depicted in Scheme 7.

Hydrogenations were carried out in a stainless steel autoclave on a 1-mmol scale using 1 mol % of catalyst. The conversions were determined by ^{1}H NMR spectroscopy and the enantiomeric excesses of the products by chiral GC or HPLC. The results are given in Table 2.

In all cases, complete conversion was obtained. The catalytic system based on SYNPHOS® ligand gave high enantiomeric excesses for the reduction of β-keto esters (**7a**−**e**) under 4 bar of hydrogen at 50 °C, providing the corresponding substituted β-hydroxy esters with enantiomeric excesses ranging from 97%, for the aromatic compound **7e**, to > 99% for aliphatic compounds **7a**−**d**. Ruthenium-mediated hydrogenation is known to give poor values of *ee* for fluorous substrates **7f** and **7g**, even at high temperature (99 °C),[20] but SYNPHOS® ligand displayed higher enantioselectivities (49% and 63%, respectively) than BINAP ligand (23% and 44%, respectively) under the same conditions.[20] Enantioselectivities for the reduction of other ketone substrates also turned out to be very high. α-Hydroxy esters, resulting from the asymmetric hydrogenation of compounds **8**, were obtained with enantiomeric purities of 92−94% under 20 bar of hydrogen at 50 °C, except for thienyl compound **8c**, which gave a moderate 71% *ee*, under 10 bar

Table 2. Hydrogenation results

Substrate[a]	Ligand configuration	Solvent	pH_2 [bar]	T [°C]	t [h]	*ee*[b] (config.)
7a	(*R*)	MeOH	4	50	24	> 99% (*R*)
7b	(*R*)	MeOH	4	50	24	> 99% (*R*)
7c	(*R*)	EtOH	4	50	24	> 99% (*R*)
7d	(*R*)	EtOH	4	50	24	> 99% (*R*)
7e	(*R*)	EtOH	10	80	24	97% (*S*)
7f	(*S*)	EtOH	10	99	1	49% (*R*)
7g	(*S*)	EtOH	10	99	3	63% (*R*)
8a	(*S*)	EtOH	20	50	24	94% (*S*)
8b	(*R*)	MeOH	20	50	24	92% (*R*)
8c	(*R*)	EtOH	10	80	24	71% (*R*)
9a	(*S*)	MeOH	30	65	7	97% (*S*)
9b	(*R*)	MeOH	30	30	24	98% (*R*)
9c	(*R*)	EtOH	20	50	24	> 99% (*S*)
9d	(*R*)	MeOH	20	30	72	> 99% (*R*, *R*), *de* > 99%
10a	(*S*)	MeOH	5	50	24	86% (*S*)
10b	(*S*)	MeOH	2	50	24	91% (*S*)

[a] All conversions were 100%, according to ^{1}H NMR spectroscopy. [b] See Exp. Sect. for method of *ee* determination.

 © 2003 Wiley-VCH Verlag GmbH & Co. KGaA, Weinheim

of hydrogen at 80 °C. Various functionalized ketones, like hydroxyacetone **9a**, thioketone **9b**, β-keto phosphonate **9c**, and 1,3-diketone **9d**, were also hydrogenated with values of *ee* greater than 97%. Finally, asymmetric hydrogenation of ethylenic substrates were satisfactory [i.e., 86% *ee* for methyl (*Z*)-2-*N*-acetamidocinnamate (**10a**) and 91% *ee* for dimethyl itaconate (**10b**)].

Interestingly, these complexes were also efficient using a substrate:catalyst ratio of up to 10000 under 20 bar of hydrogen at 50 °C, providing pure methyl (3*R*)-hydroxybutanoate on a multigram scale,[21] as shown in Scheme 8.

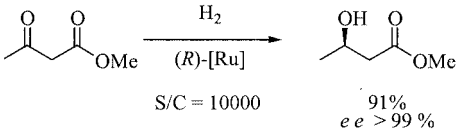

Scheme 8

Molecular Modeling

In addition to the crystal structure of the SYNPHOSO_2/DBTA complex, structural information about SYNPHOS® and other atropisomeric diphosphanes was obtained from a molecular modeling study. We minimized the structures of several complexes by CAChe MM2 calculations. We selected [(diphosphane)$PdCl_2$] (Figure 2) and [(diphosphane)RuHCl(substrate)] (Figure 3) as model complexes for our study.

In the palladium complex, two of the phenyl rings have a pseudo-axial orientation and apparent arene−arene interactions with the parallel benzodioxane moiety. The other two phenyl units have a pseudo-equatorial orientation. Most geometrical information in this model is similar to that previously reported for X-ray crystal structures of such complexes.[22]

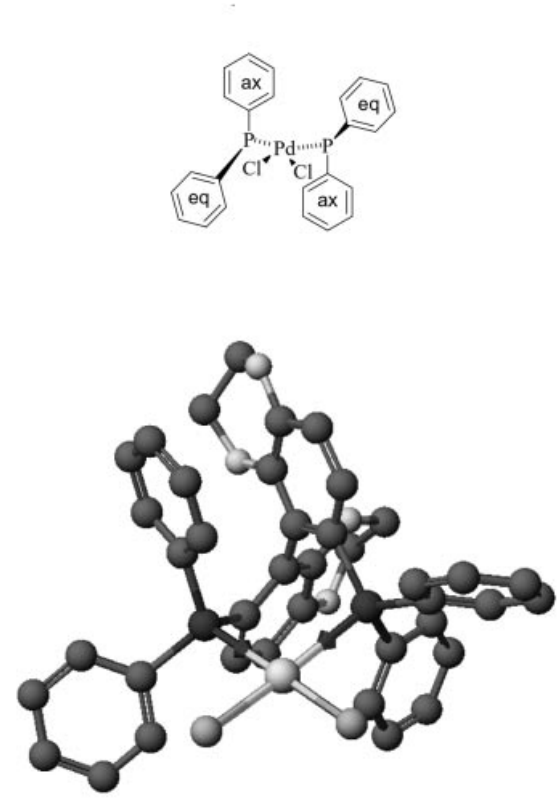

Figure 2. [(*S*)-SYNPHOS®]$PdCl_2$ complex (CAChe MM2 representation)

The ruthenium model in Figure 3 represents an intermediate complex formed between RuHCl[(*S*)-SYNPHOS®]

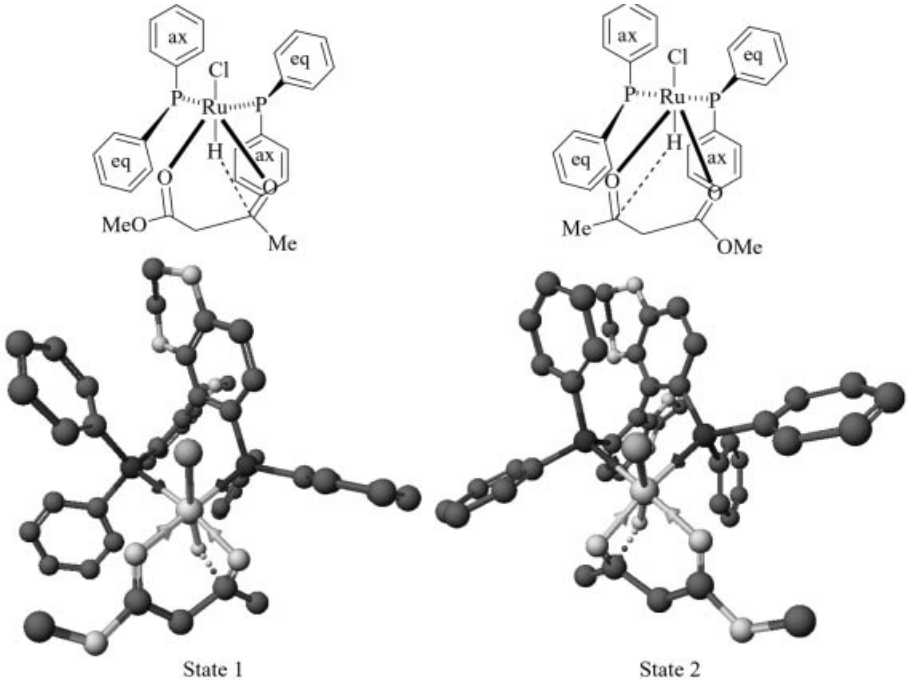

Figure 3. Diastereomeric intermediates {[(*S*)-SYNPHOS®]RuHCl·$CH_3COCH_2COOCH_3$} (CAChe MM2 representation)

 © 2003 Wiley-VCH Verlag GmbH & Co. KGaA, Weinheim

and methyl acetoacetate, in which the β-keto ester substrate is chelated to the ruthenium center through the two carbonyl functions. Very recently, ruthenium(alkoxide) intermediates have been identified as catalytic species in ruthenium-mediated asymmetric ketone hydrogenation.[23] Thus, we tried to represent the hydrogenation transition state by creating a weak bond between the hydrogen atom of the Ru-monohydride complex and the carbon atom of the ketone moiety in the substrate. As observed in the palladium complex, the phenyl rings adopt a pseudo-axial/equatorial orientations. There are two possible diastereoisomeric transition states for this complex, depending on the orientation of the substrate (coordination of the *re* or *si* face of the keto group).

It is well established that steric properties influence the selectivities in transition metal-catalyzed reactions dramatically.[8,9,24] We were interested in evaluating the dihedral angle (θ) corresponding to the axially chiral biphenyl moiety (Figure 4), in a preliminary study of the steric effects of the ligands on catalyst reactivities.

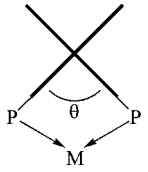

Figure 4. Dihedral angle

Having evaluated the dihedral angle (θ), we decided to compare the geometric properties of two atropisomeric diphosphane ligands, BINAP and MeO-BIPHEP, with SYNPHOS®. We have determined the dihedral angles in their corresponding minimized structures. The results are shown in Table 3.

In all the calculated structures — i.e., the free diphosphane, the palladium complex, and the two states of the ruthenium complex — the dihedral angles decrease in the following order: BINAP, MeO-BIPHEP, and SYNPHOS®. These results are in agreement with those obtained by Saito on the minimized structures of Ikariya-type ruthenium complexes with BINAP and MeO-BIPHEP ligands ($[NH_2Et_2]^+[\{RuCl(BINAP)\}_2(\mu\text{-}Cl)_3]^-$).[9]

We then determined the relative energies of the models of the intermediates in the ruthenium-mediated hydrogenations. The results are shown in Table 4. For each ligand, the difference in energy is around 2 kcal/mol and State 1 always has the lowest energy.[25] State 1 can be defined as the favored transition state in this reaction.

With the (*S*)-configured ligands, which hinder the upper-right and bottom-left space sections in the chiral array of

Table 3. Dihedral angles of minimized structures

Ligand	Dihedral angle (°)			
	Diphosphane	Palladium complex	Ruthenium complex	
			State 1	State 2
BINAP	86.2	79.1	79.5	78.1
MeO-BIPHEP	72.3	75.1	75.7	75.3
SYNPHOS®	70.7	70.2	75.4	73.2

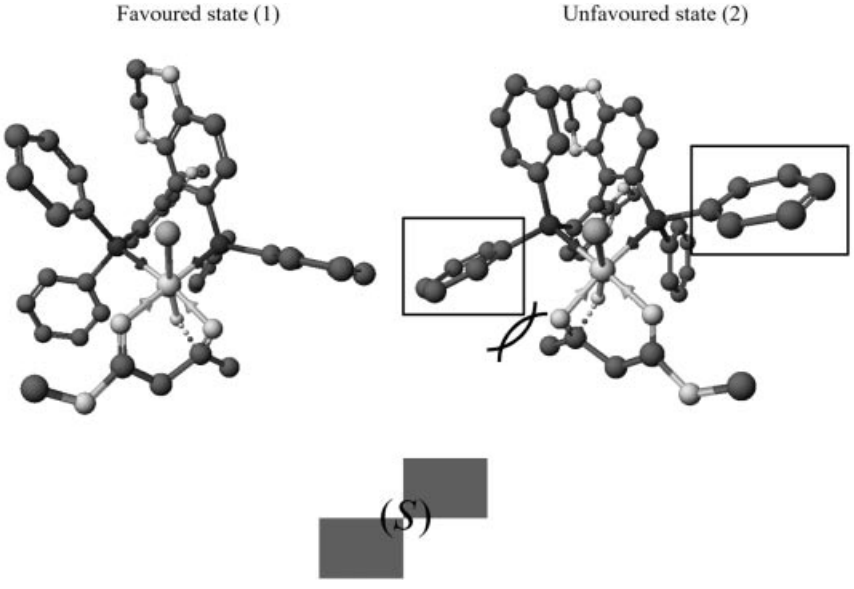

Figure 5. Quadrants diagram for (*S*)-SYNPHOS®

 © 2003 Wiley-VCH Verlag GmbH & Co. KGaA, Weinheim

Table 4. Relative energies of the diastereoisomeric intermediates [[(*S*)-SYNPHOS®]RuHCl·$CH_3COCH_2COOCH_3$]

Ligand	Relative energy (kcal/mol)	
	State 1	State 2
BINAP	−51.87	−49.40
MeO-BIPHEP	−29.27	−27.20
SYNPHOS®	−27.55	−23.12

the ruthenium complex (Figure 5), coordination of the *si* face of the keto group affords the sterically less-hindered intermediate. The modeling results are in agreement with the stereochemical model of the quadrants diagram developed for the reduction of carbonyl derivatives with ruthenium−arylphosphane catalysts,[6a] as depicted in Scheme 9.

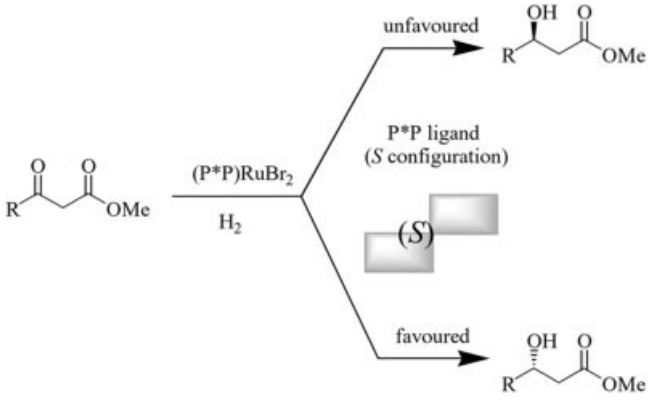

Scheme 9. Sense of enantioselectivity in the asymmetric Ru-catalyzed hydrogenation of β-keto esters

Correlation between Molecular Modeling and Enantioselectivities

For several years now, chemists at Hoffmann-La Roche[26] and in our group[20,27] have found that MeO-BIPHEP ligand is sometimes more efficient than BINAP ligand in the ruthenium-mediated asymmetric hydrogenation of functionalized prochiral ketones. Having in hand molecular modeling information about three atropisomeric diphosphane ligands, BINAP, MeO-BIPHEP, and SYNPHOS®, we decided to determine the influence that the dihedral angles have on the enantioselectivities of the asymmetric hydrogenations of several substrates. The results are shown in Figure 6. Several substrates were hydrogenated under strictly the same conditions for each of the three ligands. We were pleased to see that the highest values of *ee* were always obtained with SYNPHOS® ligand, which has the lowest dihedral angle.

As illustrated in Figure 7, the smaller the dihedral angle, the higher the interaction between the bulky equatorial phenyl group and the R group of the substrate. Thereby, the enantioselectivity is enhanced, thanks to this higher chiral differentiation.

Conclusions

We have reported here the synthesis of SYNPHOS®,[28] a new, atropisomeric, chiral diphosphane ligand, and its use in ruthenium-catalyzed asymmetric hydrogenations. Thanks to this efficient transition metal-catalyzed reaction, we have access to a wide range of chiral building blocks, such as optically active alcohols, with values of *ee* of up to 99%. We have also studied the influence of the steric properties

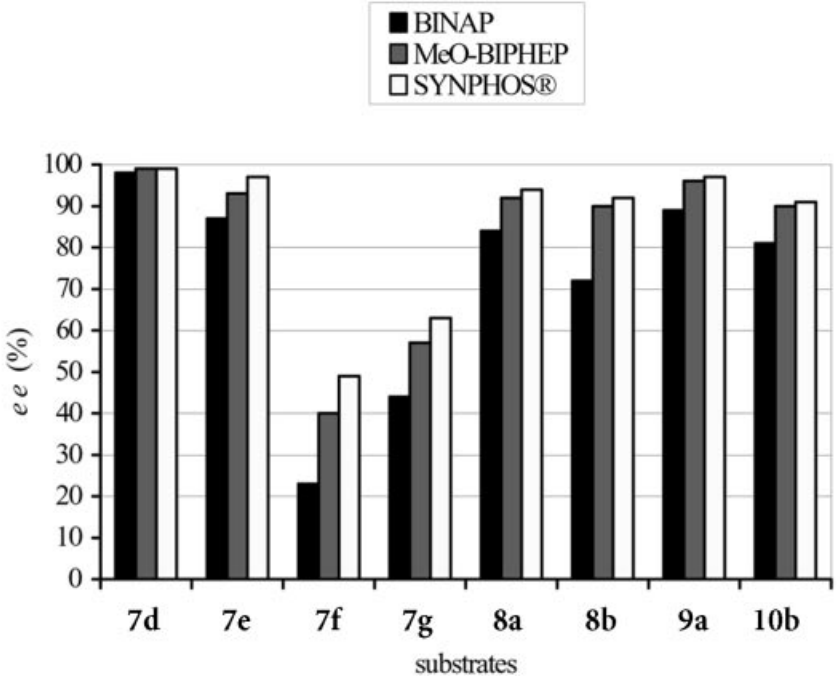

Figure 6. Correlation between θ and *ee* in the asymmetric ruthenium-mediated hydrogenation

 © 2003 Wiley-VCH Verlag GmbH & Co. KGaA, Weinheim

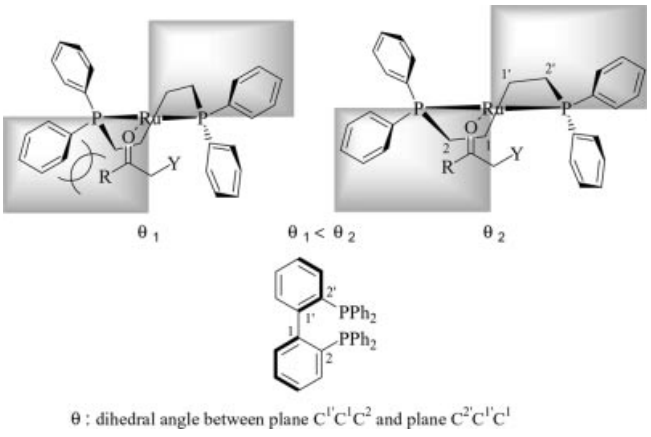

Figure 7. Steric hindrance and dihedral angles

of the diphosphanes chelated to the ruthenium catalysts. With CAChe MM2 calculations, we have evaluated a representative factor of atropisomeric diphosphanes (i.e., the dihedral angle corresponding to the axial chirality of the biphenyl moiety). This steric parameter plays a crucial role in the enantiofacial recognition, which exerts a dramatic effect on the enantioselectivities of ruthenium-mediated asymmetric hydrogenation reactions: a narrower dihedral angle provides a higher chiral differentiation. We compared three atropisomeric diphosphane ligands that were expected to have similar electronic properties. Evaluation of the electronic properties of these ligands and the design of new atropisomeric diphosphanes with similar geometric properties, but with strongly different electronic properties, are currently in progress. Such developments should assist in the discovery of new atropisomeric diphosphane ligands and an understanding of their steric and electronic properties, which will be published in due course.

Experimental Section

General Remarks: ^{1}H NMR spectra were recorded on a Bruker AC 200 at 200 MHz or on an Avance 400 at 400 MHz, ^{13}C NMR spectra were recorded on a Bruker AC 200 at 50 MHz, and ^{31}P NMR spectra were recorded on an Avance 400 at 162 MHz. Chemical shifts (δ) are reported in ppm downfield relative to internal Me_4Si or external H_3PO_4. Coupling constants (*J*) are reported in Hz and refer to apparent peak multiplicities. Mass spectra were determined on a Ribermag instrument. Ionization was obtained either by electronic impact (EI) or chemical ionization with ammonia (DCI/NH_3), or by electrospray (ESI) for compounds (−)-(*S*)-**6** and (+)-(*R*)-**6**. Optical rotations were measured on a Perkin−Elmer 241 polarimeter at 589 nm (sodium lamp). Melting points (m.p.) were determined on a Kofler melting point apparatus. Gas chromatographic analyses were performed on a Hewlett−Packard 5890 serie II instrument, connected to a Merck D-2500 or D-2000 integrator, using a flame-ionization detector; enantiomeric excesses were determined on chiral capillary columns: Lipodex A, Hydrodex-β-6-TBDM, Chirasil-Val, or Megadex 5. HPLC analyses of compound **5** were conducted with a Waters 600 system, using a Daicel Chiralcel chiral stationary-phase column: OD-H hexane/2-propanol, 90:10. All reactions were carried out under an atmosphere of argon unless otherwise noted.

6-Bromo-2,3-dihydro-1,4-benzodioxine (2): 2,3-Dihydro-1,4-benzodioxine (35 g, 0.257 mol) and 200 mL of anhydrous DMF were mixed at 0 °C. *N*-Bromosuccinimide (54.9 g, 0.308 mmol) was added in portions at 0 °C. After stirring for 24 h at room temperature, the solution was concentrated in vacuo. The residue was filtered and the precipitate was washed with CH_2Cl_2 (50 mL). The resulting filtrate was treated with 30% aqueous Na_2SO_3 solution (50 mL), washed with brine, and dried over $MgSO_4$. After evaporation and distillation (b.p. = 99 °C, 0.4 Torr), compound **2** was obtained as a colorless oil (54 g, quantitative). ^{1}H NMR ($CDCl_3$): δ = 4.25 (s, 4 H), 6.74 (d, *J* = 8.5 Hz, 1 H), 6.93 (dd, *J* = 8.5, 2.3 Hz, 1 H), 7.02 (d, *J* = 2.3 Hz, 1 H) ppm. ^{13}C NMR ($CDCl_3$): δ = 64.1, 112.7, 118.5, 120.1, 124.1, 142.8, 144.2 ppm. MS: *m*/*z* = 214.

(2,3-Dihydro-1,4-benzodioxin-6-yl)diphenylphosphane Oxide (3): *n*BuLi (25.6 mL, 2.2 M solution in hexane, 56.3 mmol) was added dropwise to a solution of 6-bromo-2,3-dihydro-1,4-benzodioxine **2** (11 g, 51.1 mmol) in dry THF (30 mL) at −78 °C over 10 min. The resulting suspension was stirred for an additional 1 h at −78 °C, and then freshly distilled Ph_2PCl (10.4 mL, 56.3 mmol) was added dropwise at such a rate that the reaction temperature did not exceed −60 °C. The orange solution was warmed to 0 °C within 2 h, during which time the solution turned red, then yellow, and then quenched with saturated aqueous NH_4Cl (20 mL). The organic layer was separated, washed with brine, dried over $MgSO_4$, filtered, and the solvents were evaporated. The solid residue was washed with hot hexane and a light-yellow solid was collected by filtration. This solid was suspended in MeOH (60 mL) and 30% aqueous H_2O_2 (8 mL) was added dropwise at 0 °C. After stirring for 1 h at room temperature, the resulting clear solution was treated with 30% aqueous Na_2SO_3 (14 mL), stirred for an additional 1 h, and then treated with 1 N aqueous HCl (9 mL). The resulting mixture was concentrated in vacuo to remove MeOH and the aqueous residue was extracted with CH_2Cl_2 (50 mL). The organic layer was dried over $MgSO_4$, filtered, and the solvents were evaporated. The yellow oily residue crystallized on standing and the solids were washed with hot hexane to yield **3** as a white solid (15.5 g, 90%). M.p. 150−155 °C. ^{1}H NMR ($CDCl_3$): δ = 4.26 (m, 4 H), 6.95 (dd, *J* = 11.8, 3.1 Hz, 1 H), 7.09−7.18 (m, 2 H), 7.42−7.54 (m, 6 H), 7.61−7.72 (m, 4 H) ppm. ^{13}C NMR ($CDCl_3$): δ = 64.1, 64.4, 117.6 (d, *J* = 14.6 Hz), 121.2 (d, *J* = 12.1 Hz), 125.5 (d, *J* = 10.3 Hz), 128.2, 128.4, 131.7, 131.8, 132.0, 133.6, 143.3, 146.7 ppm. ^{31}P NMR ($CDCl_3$): δ = 30.10 ppm. MS: *m*/*z* = 335.

(5-Iodo-2,3-dihydro-1,4-benzodioxin-6-yl)diphenylphosphane Oxide (4): *t*BuLi (2 mL, 1.5 M solution in pentane, 3 mmol) was added dropwise to a solution of **3** (1 g, 2.9 mmol) in dry THF (25 mL) at −100 °C. Over a period of 30 min, the reaction temperature was warmed to −70 °C, and the resulting red solution was stirred for an additional 3 h at this temperature. I_2 was then added at −70 °C and a beige precipitate was formed. The reaction temperature was raised to 0 °C over 2 h, during which time the mixture became a clear red solution. This solution was treated with 20% aqueous Na_2SO_3 (5 mL). The organic layer was washed with brine, dried over $MgSO_4$, filtered, and then the solvents were evaporated to yield crude **4** as a yellow solid (1.34 g, containing 25% of starting material). ^{1}H NMR ($CDCl_3$): δ = 4.31 (m, 4 H), 6.69 (dd, *J* = 12.7, 8.7 Hz, 1 H), 7.81 (dd, *J* = 8.6, 2.8 Hz, 1 H), 7.47−7.58 (m, 6 H), 7.63−7.77 (m, 4 H) ppm. ^{31}P NMR ($CDCl_3$): δ = 34.42 ppm. MS: *m*/*z* = 462.

[2,3,2′,3′-Tetrahydro-5,5′-bi(1,4-benzodioxin)-6,6′-diyl]bis(diphenylphosphane Oxide), SYNPHOSO$_2$ (5). Method A

 © 2003 Wiley-VCH Verlag GmbH & Co. KGaA, Weinheim

(Oxidative Coupling): *t*BuLi (65 mL, 1.5 M solution in pentane, 90 mmol) was added dropwise to a solution of **3** (30 g, 87 mmol) in dry THF (600 mL) at −100 °C. Over a period of 30 min, the reaction temperature was raised to −70 °C, and the resulting red solution was stirred for an additional 3 h at this temperature. Anhydrous $FeCl_3$ (19.8 g, 122 mmol) was then added in one portion under a flow of argon at −70 °C. The reaction temperature was raised quickly to 10 °C and the brown mixture was stirred overnight at room temperature. The solution was concentrated in vacuo, and the brown residue was diluted with CH_2Cl_2 (500 mL) and treated with 1 N aqueous NaOH (50 mL). After stirring for 30 min, the resulting suspension was filtered through celite and the filter cake was washed with CH_2Cl_2 (100 mL). The organic layer was washed with water, brine, dried over $MgSO_4$, filtered, and the solvents were evaporated. The resulting brown solid, containing 50% of starting material **3**, was dissolved in $CHCl_3$ (150 mL) and a solution of racemic dibenzoyltartaric acid (15.8 g, 44 mmol) in EtOAc (180 mL) was added. In a few minutes, a precipitate was formed. After filtration (the filtrate was concentrated in vacuo to give unchanged started material **3** (15 g, 50%) as a pale yellow solid), the solids were suspended in CH_2Cl_2 (200 mL) and treated with 1 N aqueous KOH (100 mL). After stirring for 30 min, the clear organic layer was separated, washed with water, brine, dried over $MgSO_4$, filtered, and then the solvents were evaporated to afford pure **5** (15 g, 50%) as a white solid. M.p. > 260 °C. ^{1}H NMR ($CDCl_3$): δ = 3.42 (m, 2 H), 3.70 (m, 2 H), 3.92 (m, 2 H), 4.06 (m, 2 H), 6.64 (dd, *J* = 13.3, 8.5 Hz, 2 H), 6.77 (dd, *J* = 8.5, 3.1 Hz, 2 H), 7.26−7.31 (m, 4 H), 7.35−7.55 (m, 12 H), 7.65−7.70 (m, 4 H) ppm. ^{13}C NMR ($CDCl_3$): δ = 63.3, 63.9, 115.9 (d, *J* = 14.6 Hz), 121.2, 124.5, 127.7, 127.9, 130.8, 132.1, 132.2, 132.4, 135.5, 141.0, 145.8 ppm. ^{31}P NMR ($CDCl_3$): δ = 30.97 ppm. MS: *m*/*z* = 670. HRMS: calcd. for $C_{40}H_{32}O_6P_2$ [M + H] 671.1752; found 671.1755.

Method B (Ullmann-Type Coupling): A mixture of crude **4** (1.3 g, containing 25% of **3**, 2.1 mmol) and activated copper (540 mg, 8.4 mmol) in anhydrous DMF (10 mL) was heated at 140 °C for 4 h. The solvent was evaporated and the residue was treated for 5 min with hot CH_2Cl_2 (10 mL). The solids were filtered and washed with CH_2Cl_2 (10 mL). The filtrate was washed with a saturated aqueous NH_4Cl solution (5 mL), dried over $MgSO_4$, and concentrated. The solid residue was purified by silica gel chromatography (CH_2Cl_2/MeOH, 98:2) and a white solid was obtained (500 mg, 70% based on the amount of **4**). All analytical data were identical to those of compound **5**.

Resolution of SYNPHOSO$_2$. Method A: A solution of (−)-*O*,*O*-dibenzoyltartaric acid (5.64 g, 14.9 mmol) in EtOAc (260 mL) was added to a stirred solution of *rac*-SYNPHOSO$_2$ **5** (10 g, 14.9 mmol) in $CHCl_3$ (100 mL). After a few minutes, a precipitate had formed. After filtration (the filtrate was stored for the recovery of the other enantiomer), the solids were suspended in CH_2Cl_2 (200 mL) and treated with 1 N aqueous KOH (100 mL). After stirring for 30 min, the clear organic layer was separated, washed with water, brine, dried over $MgSO_4$, filtered, and the solvents were evaporated to afford enantiomerically enriched (−)-(*S*)-**5**. The operation was repeated four times and enantiomerically pure (−)-(*S*)-**5** (*ee* > 99.9% according to HPLC) was obtained as a white solid (3.5 g, 70% based on theory). M.p. > 260 °C. $[\alpha]_D$ = −142 (*c* = 1, $CHCl_3$). All other analytical data were identical to those of compound **5**.

The combined filtrates were concentrated under vacuum and treated as described above (1 N KOH and usual workup). The resulting white solid (6.2 g, 9.2 mmol) was then treated, in the same manner, with (*D*)-(+)-dibenzoyltartaric acid (3.5 g, 9.2 mmol). The operation was repeated as above and finally (+)-(*R*)-**5** (3.5 g, 70% based on theory, *ee* > 99.9% according to HPLC) was obtained as a white solid. $[\alpha]_D$ = +143 (*c* = 1, $CHCl_3$). All other analytical data were identical to those of compound **5**.

Method B: A solution of *rac*-SYNPHOSO$_2$ **5** (26.15 g, 39 mmol) and (−)-*O*,*O*-dibenzoyltartaric acid (14.76 g, 39 mmol) in CH_2Cl_2 (500 mL) was stirred at room temperature and a white precipitate formed within a few minutes. The solids were filtered (the filtrate was stored for the recovery of the other enantiomer) and an aliquot of the resulting white solid was suspended in CH_2Cl_2 (2 mL) and treated with 1 N aqueous KOH (1 mL). After stirring for 30 min, the clear organic layer was separated, washed with water, brine, dried over $MgSO_4$, filtered, and the solvents were evaporated to afford a white solid (*ee* = 91% (+)-(*R*), according to HPLC). The solids were suspended once again in CH_2Cl_2 (200 mL), the mixture was filtered (the filtrate was stored for the recovery of the other enantiomer). The resulting white solid (18.7 g, 17.8 mmol) was suspended in CH_2Cl_2 (200 mL) and treated with 1 N aqueous KOH (100 mL). After stirring for 30 min, the clear organic layer was separated, washed with water, brine, dried over $MgSO_4$, filtered, and the solvents were evaporated to afford enantiopure (+)-(*R*)-**5** (11.9 g, 91% based on theory, *ee* > 99.9% according to HPLC) as a white solid. $[\alpha]_D$ = +143 (*c* = 1, $CHCl_3$). All other analytical data were identical to those of compound **5**.

The combined filtrates were concentrated under vacuum and treated as described above (1 N KOH and usual workup). The resulting white solid (14.2 g, 21.2 mmol) was then treated, in the same manner, with (*D*)-(+)-dibenzoyltartaric acid (8.00 g, 21.2 mmol) and finally (−)-(*S*)-**5** (11.6 g, 89% based on theory, *ee* > 99.9% according to HPLC) was obtained as a white solid. $[\alpha]_D$ = −143 (*c* = 1, $CHCl_3$). All other analytical data were identical to those of compound **5**.

[2,3,2′,3′-Tetrahydro-5,5′-bi(1,4-benzodioxin)-6,6′-diyl]bis-(diphenylphosphane), SYNPHOS® (6): Tributylamine (4.24 mL, 17.90 mmol) and trichlorosilane (1.56 mL, 14.80 mmol) were added to a suspension of **5** (1 g, 1.48 mmol) in dry xylene (10 mL). The resulting mixture was heated at 140 °C overnight. After cooling to room temperature, degassed 4 N aqueous NaOH (10 mL) was added dropwise and the mixture was stirred for 30 min. Dry CH_2Cl_2 (30 mL) was added, the organic layer was washed with degassed distilled water (10 mL) and degassed brine (10 mL), and then concentrated in vacuo. MeOH (20 mL) was added and a white precipitate formed. The solids were filtered under argon and dried in vacuo for 3 h to afford SYNPHOS® **6** (860 mg, 91%) as a white solid.

(−)-(*S*)-SYNPHOS® 6: M.p. > 260 °C. $[\alpha]_D$ = −44 (*c* = 0.1, C_6H_6). ^{1}H NMR ($CDCl_3$): δ = 3.35 (m, 2 H), 3.83 (m, 4 H), 4.13 (m, 2 H), 6.62 (dd, *J* = 8, 3 Hz, 2 H), 6.85 (d, *J* = 8 Hz, 2 H), 7.05−7.10 (m, 4 H), 7.20−7.25 (m, 8 H), 7.27−7.32 (m, 8 H) ppm. ^{31}P NMR ($CDCl_3$): δ = −14.30 ppm. MS (ESI): *m*/*z* = 639.6 ([M + H]$^+$). HRMS: calcd. for $C_{40}H_{32}O_4P_2$ [M + H] 639.1854; found 639.1844.

(+)-(*R*)-SYNPHOS® 6: M.p. > 260 °C. $[\alpha]_D$ = +44 (*c* = 0.1, C_6H_6). All other analytical data were identical to those of (−)-(*S*)-SYNPHOS® **6**.

Typical Procedure for Asymmetric Hydrogenation: (*S*)-SYNPHOS® (7.1 mg, 0.011 mmol) and [(COD)Ru{η^3-$(CH_2)_2CCH_3$}$_2$] (3.2 mg, 0.01 mmol) were placed in a 10 mL flask, and degassed anhydrous acetone (1 mL) was added dropwise. A methanolic solution of HBr (122 μL, 0.18 M) was added dropwise to the suspension. The reaction mixture was stirred at room temperature for about 30 min and

 © 2003 Wiley-VCH Verlag GmbH & Co. KGaA, Weinheim

an orange suspension was formed. The solvent was removed under vacuum. The brown solid residue was used without further purification as a catalyst for the hydrogenation reaction of the desired substrate (1 mmol) in MeOH or EtOH (2 mL). The reaction vessel was placed in a 500 mL stainless steel autoclave, which was pressurized at the desired pressure and warmed to the desired temperature for 24 h. The methanol was concentrated and the crude product was passed through a short pad of silica gel (cyclohexane/EtOAc, 1:1). Conversion and *ee* were determined by ^{1}H NMR spectroscopy and chiral GC, respectively.

X-ray Crystallographic Study: Details are listed in Table 5. CCDC-207263 contains the supplementary crystallographic data for this paper. These data can be obtained free of charge at www.ccdc.cam.ac.uk/conts/retrieving.html [or from the Cambridge Crystallographic Data Centre, 12, Union Road, Cambridge CB2 1EZ, UK; Fax: (internat.) +44−1223/336−033; E-mail: deposit@ccdc.cam.ac.uk].

Table 5. Crystal data for (−)-SYNPHOSO$_2$/(−)-DBTA

Empirical formula	$C_{58}H_{44}O_{14}P_2$
Crystal class	monoclinic
Space group	*C*2
a (Å), α (°)	24.796(4), 90
b (Å), β (°)	8.460(2), 117.70(2)
c (Å), γ (°)	13.521(3), 90
Volume (Å^3)	2511(1)
Z	2
Radiation	Mo-K_α
Wavelength (Å)	0.710690
Density	1.36
M (g mol^{-1})	1026.92
μ (cm^{-1})	1.57
Temperature (K)	295
Size (mm)	0.3 × 0.3 × 0.6
Color	colorless
Shape	stick
Diffractometer	Enraf−Nonius
Scan type	2Θ/Ω
Reflections measured	2418
Independent reflections	2192
$R_{int.}$	0.02
$\Theta_{min.,max.}$	125.00
$h_{min.}$, $h_{max.}$	0, 29
$k_{min.}$, $k_{max.}$	0, 10
$l_{min.}$, $l_{max.}$	−16, 14
Decay	0.023
Refinement on *F*	
R factor	0.0495 $R = \Sigma\|\|F_o\| - \|F_c\|\|/\Sigma\|F_o\|$
Weighted *R* factor	0.0645 $Rw^* = [\Sigma w (\|\|F_o\| - \|F_c\|\|)^2 / \Sigma w F_o^2]^{1/2}$
$\Delta\delta_{min.}$ (e/Å^3)	−0.21
$\Delta\delta_{max.}$ (e/Å^3)	0.42
Reflections used	1839
σ(*I*) limit	1.50
Number of parameters	299
Goodness of fit	1.003
Weighting scheme of the form	$w = w'\{1 - [(\|\|F_o\| - \|F_c\|\|)/6\sigma(F_o)]^2\}^2$ with $w' = 1/\Sigma_r A_r T_r(X)$ with coefficients 3.19, 1.59 and 2.51 for a Chebychev series for which $X = F_c/F_{c,max}$.

Acknowledgments

CNRS and SYNKEM S.A.S. are gratefully acknowledged for a doctoral fellowship. We deeply thank Dr A. Solladié-Cavallo, from the Department of Fine Organic Chemistry (ECPM, Strasbourg, France), for her kind permission to use molecular modeling facilities. We also thank Dr R. Schmid (Hoffmann-La Roche) for a generous gift of (*S*)- and (*R*)-MeO-BIPHEP.

[1] H. B. Kagan, in *Comprehensive Asymmetric Catalysis* (Eds.: E. N. Jacobsen, A. Pfaltz, H. Yamamoto), Springer-Verlag, Berlin, **1999**, Vol. I, Chap. 2, p. 9.
[2] For a review, see: R. Noyori, H. Takaya, *Acc. Chem. Res.* **1990**, *23*, 345−350.
[3] R. Schmid, E. A. Broger, M. Cereghetti, Y. Crameri, J. Foricher, M. Lalonde, R. K. Müller, M. Scalone, G. Schoettel, U. Zutter, *Pure Appl. Chem.* **1996**, *68*, 131−138.
[4] T. Saito, N. Sayo, Z. Xiaoyaong, T. Yokozawa, EP 0850945, **1998**.
[5] For a review on axially chiral bidentate ligands, see: M. McCarthy, P. J. Guiry, *Tetrahedron* **2001**, *57*, 3809−3844.
[6] [6a] R. Noyori, in *Asymmetric Catalysis in Organic Synthesis*, Wiley & Sons, New York, **1994**, p. 1−93. [6b] R. Noyori, *Tetrahedron* **1994**, *50*, 4259−4292. [6c] T. Ohkuma, M. Kitamura, R. Noyori, in *Catalytic Asymmetric Synthesis* (Ed.: I. Ojima), **2000**, p. 1−110. [6d] R. Noyori, T. Ohkuma, *Angew. Chem. Int. Ed.* **2001**, *40*, 40−73. [6e] R. Noyori, *Angew. Chem. Int. Ed.* **2002**, *41*, 2008−2022. [6f] J.-P. Genêt, *Pure Appl. Chem.* **2002**, *74*, 77−83.
[7] R. Schmid, J. Foricher, M. Cereghetti, P. Schönholzer, *Helv. Chim. Acta* **1991**, *74*, 370−389.
[8] Z. Zhang, H. Qian, J. Longmire, X. J. Zhang, *J. Org. Chem.* **2000**, *65*, 6223−6226.
[9] T. Saito, T. Yokozawa, T. Ishizaki, T. Moroi, N. Sayo, T. Miura, H. Kumobayashi, *Adv. Synth. Catal.* **2001**, *343*, 264−267, and references cited therein.
[10] [10a] P. Guerreiro, V. Ratovelomanana-Vidal, J.-P. Genêt, P. Dellis, *Tetrahedron Lett.* **2001**, *42*, 3423−3426. [10b] G. Michaud, M. Bulliard, L. Ricard, J.-P. Genêt, A. Marinetti, *Chem. Eur. J.* **2002**, *8*, 3327−3330.
[11] [11a] S. Duprat de Paule, N. Champion, V. Vidal, J.-P. Genêt, P. Dellis, French patent 0112499, **2001**, PCT FR02/03146. [11b] See also: C. C. Pai, Y. M. Li, Z. Y. Zhou, A. S. C. Chan, *Tetrahedron Lett.* **2002**, *43*, 2789−2792.
[12] J. M. Brown, S. C. Woodward, *J. Org. Chem.* **1991**, *56*, 6803−6809.
[13] H. Brunner, W. Pieronczyk, B. Schönhammer, K. Streng, I. Bernal, J. Korp, *Chem. Ber.* **1981**, *114*, 1137−1149.
[14] [14a] S. Otsuka, T. Nakamura, T. Kano, K. Tani, *J. Am. Chem. Soc.* **1971**, *93*, 4301−4303. [14b] K. Tani, L. D. Brown, J. Ahmed, J. A. Ibers, M. Yokota, T. Nakamura, S. Otsuka, *J. Am. Chem. Soc.* **1977**, *99*, 7876−7886.
[15] [15a] N. K. Roberts, S. B. Wild, *J. Am. Chem. Soc.* **1979**, *101*, 6254−6260. [15b] N. K. Roberts, S. B. Wild, *J. Chem. Soc., Dalton Trans.* **1979**, 2015−2021.
[16] [16a] A. Miyashita, A. Yasuda, H. Takaya, K. Toriumi, T. Ito, T. Souchi, R. Noyori, *J. Am. Chem. Soc.* **1980**, *102*, 7932−7934. [16b] R. Noyori, M. Ohta, Y. Hsiao, M. Kitamura, J. Ohta, H. Takaya, *J. Am. Chem. Soc.* **1986**, *108*, 7117−7119. [16c] R. Noyori, T. Ohkuma, M. Kitamura, H. Takaya, N. Sayo, H. Kumobayashi, S. Akutagawa, *J. Am. Chem. Soc.* **1987**, *109*, 5856−5858. [16d] M. Kitamura, T. Ohkuma, S. Inoue, N. Sayo, H. Kumobayashi, S. Akutagawa, T. Ohta, H. Takaya, R. Noyori, *J. Am. Chem. Soc.* **1988**, *110*, 629−631.
[17] [17a] T. Ikariya, Y. Ishii, H. Kawano, T. Arai, M. Saburi, S. Yoshikawa, S. Akutagawa, *J. Chem. Soc., Chem. Commun.* **1985**, 922−924. [17b] H. Kawano, T. Ikariya, Y. Ishii, M. Saburi, S. Yoshikawa, Y. Uchida, H. Kumobayashi, *J. Chem. Soc., Perkin Trans. 1* **1989**, 1571−1575.

 © 2003 Wiley-VCH Verlag GmbH & Co. KGaA, Weinheim

[18] [18a] V. Ratovelomanana-Vidal, J.-P. Genêt, *J. Organomet. Chem.* **1998**, *567*, 163−171. [18b] V. Ratovelomanana-Vidal, J.-P. Genêt, *Can. J. Chem.* **2000**, *78*, 846−851. [18c] V. Ratovelomanana-Vidal, C. Girard, R. Touati, J.-P. Tranchier, B. Ben Hassine, J.-P. Genêt, *Adv. Synth. Catal.* **2003**, *345*, 261−274.

[19] [19a] J.-P. Genêt, C. Pinel, V. Ratovelomanana-Vidal, S. Mallart, X. Pfister, M. C. Cano de Andrade, J.-A. Laffitte, *Tetrahedron: Asymmetry* **1994**, *5*, 665−674. [19b] J.-P. Genêt, C. Pinel, V. Ratovelomanana-Vidal, S. Mallart, X. Pfister, L. Bischoff, M. C. Cano de Andrade, S. Darses, C. Galopin, J.-A. Laffitte, *Tetrahedron: Asymmetry* **1994**, *5*, 675−690. [19c] J.-P. Genêt, *Reductions in Organic Synthesis*; A. C. S. Symposium Series 641, **1996**, p. 31−51.

[20] D. Blanc, V. Ratovelomanana-Vidal, J.-P. Gillet, J.-P. Genêt, *J. Organomet. Chem.* **2000**, *603*, 128−130.

[21] See Exp. Sect. for a typical procedure.

[22] [22a] For [(BINAP)$PdCl_2$], see: F. Ozawa, A. Kubo, Y. Matsumoto, T. Hayashi, E. Nishioka, K. Yanagi, K. I. Moriguchi, *Organometallics* **1993**, *12*, 4188−4196. [22b] T. Hayashi, Y. Kobori, M. Kumada, T. Higuchi, K. Hirotsu, *J. Am. Chem. Soc.* **1984**, *106*, 158−163.

[23] C. J. A. Daley, S. H. Bergens, *J. Am. Chem. Soc.* **2002**, *124*, 3680−3691.

[24] P. Dierkes, P. W. N. M. van Leeuwen, *J. Chem. Soc., Dalton. Trans.* **1999**, 1519−1529.

[25] Energy differences were quite low (2 kcal/mol), but these values are representative for two diastereoisomeric model transition states.

[26] B. Heiser, E. A. Broger, Y. Crameri, *Tetrahedron: Asymmetry* **1991**, *2*, 51−62.

[27] [27a] For thioketones, see: J.-P. Tranchier, V. Ratovelomanana-Vidal, J.-P. Genêt, S. Tong, T. Cohen, *Tetrahedron Lett.* **1997**, *38*, 2951−2954. [27b] For β-keto sulfones, see: P. Bertus, P. Phansavath, V. Ratovelomanana-Vidal, J.-P. Genêt, A. R. Touati, T. Homri, B. Ben Hassine, *Tetrahedron: Asymmetry* **1999**, *10*, 1369−1380. [27c] For phosphonic acids, see: J. C. Henry, D. Lavergne, V. Ratovelomanana-Vidal, J.-P. Genêt, I. P. Beletskaya, T. M. Dolgina, *Tetrahedron Lett.* **1998**, *39*, 3473−3476.

[28] S. Duprat de Paule, S. Jeulin, V. Ratovelomanana-Vidal, J.-P. Genêt, N. Champion, P. Dellis, *Tetrahedron Lett.* **2003**, *44*, 823−826.

Received November 14, 2002

 © 2003 Wiley-VCH Verlag GmbH & Co. KGaA, Weinheim